

# Heterogeneous photocatalysis: From water photolysis to applications in environmental cleanup

Akira Fujishima<sup>a,\*</sup>, Xintong Zhang<sup>a</sup>, Donald. A. Tryk<sup>b</sup>

<sup>a</sup>Kanagawa Academy of Science and Technology, KSP Bldg. West 614, 3-2-1 Sakado, Takatsu-ku, Kawasaki, Kanagawa 213-0012, Japan

<sup>b</sup>Department of Applied Chemistry, Faculty of Urban Environmental Sciences, Tokyo Metropolitan University, 1-1 Minami-Ohsawa, Hachiohji, Tokyo 192-0397, Japan

Available online 23 October 2006

## Abstract

Water splitting and environmental cleanup are two active fields in heterogeneous photocatalysis, which are both closely related to the research in semiconductor photoelectrochemistry since the 1960s. The present review paper will attempt to describe some of the progress and resulting achievements in these two fields, and to briefly discuss the future prospects. We will cover the major developments worldwide but will highlight work carried out in Japan over the last several years.

© 2006 International Association for Hydrogen Energy. Published by Elsevier Ltd. All rights reserved.

*Keywords:* Heterogeneous photocatalysis; Water splitting; Environmental cleanup

## 1. Introduction

Intensive studies in heterogeneous photocatalysis started three decades ago, after the discovery of the photo-induced splitting of water on TiO<sub>2</sub> electrodes [1,2]. Early studies were focused on the utilization of solar energy for the production of hydrogen as a clean fuel from water [3–5]. However, various workers also found that illuminated semiconductor particles could catalyze a wide range of interesting and useful redox reactions of organic and inorganic substrates [6]. In particular, such particles were found to completely decompose a variety of organic or inorganic compounds that were known as environment pollutants. Thenceforth, extensive studies were initiated on the environmental applications of heterogeneous photocatalysis [7–9]. During the last decade, practical applications of TiO<sub>2</sub> photocatalysts have been implemented in both indoor and outdoor environments [10,11].

The present paper will briefly trace the development of heterogeneous photocatalysis in the areas of energy storage and environmental cleanup, describe some of the progress and resulting achievements, and discuss the future prospects. We will call attention to work carried out in Japan during the last five

years but will also put this work into a global and historical context.

## 2. Photocatalytic water splitting

### 2.1. Background: photoelectrochemical water splitting

Plants harvest the electromagnetic energy from the sun and use it to sustain life, both for themselves and for the rest of the global ecosystem. During this process, they produce oxygen by oxidizing water, and they synthesize a wide variety of organic compounds by reducing carbon dioxide. Essentially, through photosynthesis, they accomplish two basic electrochemical processes: the oxidation of water and the reduction of CO<sub>2</sub>. Photoelectrochemistry provides a way to mimic photosynthesis by employing a semiconductor electrode to absorb and utilize solar energy to convert chemicals into other forms. The first work that clearly showed this possibility was the photoelectrolysis of water on TiO<sub>2</sub> electrodes [1,2].

Water photoelectrolysis was first carried out with a system in which an n-type TiO<sub>2</sub> semiconductor (rutile) electrode, which was connected through an electrical load to a platinum black counter electrode, was exposed to near-UV light (< 415 nm). When the surface of the TiO<sub>2</sub> electrode was illuminated, electrons flowed from it to the platinum counter electrode through

\* Corresponding author. Tel.: +81 044 819 2020; fax: +81 044 819 2038.

E-mail address: [fujishima@newkast.or.jp](mailto:fujishima@newkast.or.jp) (A. Fujishima).

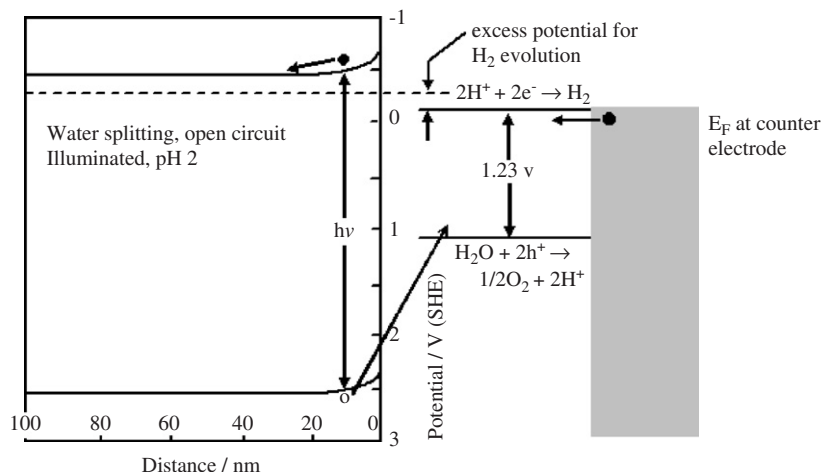


Fig. 1. Schematic representation of photoelectrochemical water electrolysis with an illuminated oxide semiconductor electrode such as  $\text{TiO}_2$  [9]. Open circuit (or small current), pH 2, illuminated conditions are shown for an oxide with an  $E_{\text{CB}}$  of  $-0.65$  V (SHE) and an  $E_{\text{VB}}$  of  $2.35$  V (SHE). At open circuit, a small excess potential ( $\sim 0.15$  V) is available for  $\text{H}_2$  evolution, assuming a reversible counter electrode.

the external circuit. The direction of the current shows that an oxidation reaction (oxygen gas evolution) occurs at the  $\text{TiO}_2$  electrode and a reduction reaction (hydrogen gas evolution) occurs at the Pt electrode.

As illustrated in Fig. 1, if the conduction band energy  $E_{\text{CB}}$  of a semiconducting electrode is higher (or more negative on the electrochemical scale) than the hydrogen evolution potential, photogenerated electrons can flow to the counter electrode and reduce protons, resulting in hydrogen gas evolution without an applied potential. The  $E_{\text{CB}}$  for rutile is very close in potential to that necessary to evolve molecular hydrogen from water. However, to achieve practical current densities, additional potential driving force is required. In these early studies, this additional driving force was supplied by use of a pH gradient: the  $\text{TiO}_2$  electrode was immersed in a more alkaline electrolyte solution and the Pt counter electrode was immersed in a more acid solution, and the two compartments were separated by porous glass plug to avoid mixing [12]. Due to the shifting of the conduction and valence bands of the  $\text{TiO}_2$  electrode higher in energy with increasing pH, the conduction band electrons that are generated by illumination of the  $\text{TiO}_2$  electrode have a sufficiently high (negative) electrochemical potential, which is sufficient to evolve hydrogen at the Pt electrode in the more acidic solution. Later, it was shown that  $\text{SrTiO}_3$ , which has a larger band gap energy and a more negative  $E_{\text{CB}}$ , is able to photoelectrolyze water directly, without a pH gradient. Similarly, other oxide semiconductors, such as the anatase form of  $\text{TiO}_2$ ,  $\text{CaTiO}_3$ ,  $\text{KTaO}_3$ ,  $\text{Ta}_2\text{O}_5$  and  $\text{ZrO}_2$ , also satisfy the  $E_{\text{CB}}$  requirement [13]. However, since these compounds all have relatively large band gap energies, the solar energy conversion efficiencies, which are based on the full solar spectrum, are rather low.

One alternative approach to capturing a greater portion of the solar spectrum is to use a dual junction or tandem system. For example, in the work of Khaselev and Turner, a solid-state tandem cell system was developed in which the semiconductor electrode consisted of a GaAs bottom layer connected to a  $\text{GaInP}_2$  top layer [14]. The  $\text{GaInP}_2$  band gap is  $1.83$  eV. The

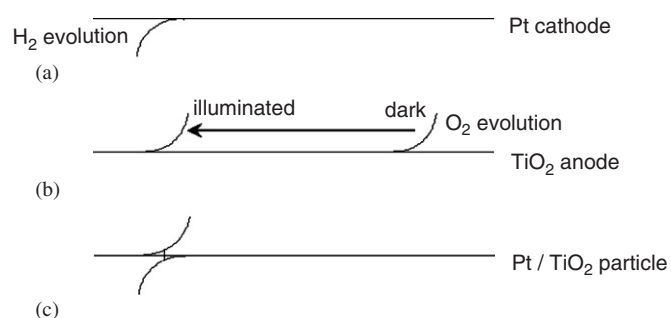


Fig. 2. Schematic diagram of hypothetical electrochemical and photoelectrochemical reactions occurring on a single Pt/ $\text{TiO}_2$  particle dispersed in water (c). For comparison, the corresponding processes occurring on (a) Pt cathode and (b) a  $\text{TiO}_2$  cathode are shown, the latter two being connected to a potentiostat as a working electrode [9].

GaAs band gap is  $1.42$  eV. The maximum solar energy conversion efficiency for this combination of band gaps is  $34\%$ .  $\text{H}_2$  is produced at the semiconductor electrode, and  $\text{O}_2$  is produced at the Pt electrode under solar illumination. This system yields  $12.4\%$  conversion efficiency for an incident light intensity of  $1190$   $\text{mW cm}^{-2}$ . The principal shortcoming of this system is the high cost of the multilayer photoelectrode.

## 2.2. Water splitting by heterogeneous photocatalysis

The principles of photoelectrochemical water splitting have also been used to guide the design of particulate systems for photocatalytic water splitting [15,16]. For example, a  $\text{TiO}_2$  particle with a small amount of Pt deposited on it is essentially a miniature photoelectrochemical cell, on which water is oxidized at the bare oxide and is reduced at the Pt-covered area to achieve the desired overall reaction (see Fig. 2). Such particulate systems have the advantage of being much simpler and less expensive to construct and use compared with the photoelectrochemical cell. Moreover, a variety of materials can be used

in particulate systems that may be difficult to prepare in single crystals or high quality polycrystalline form. Another advantage is that the electrical conductivity need not be as high as that needed for bulk electrodes. However, particulate photocatalytic systems also have the disadvantages. For example, the separation of charge carriers is not as efficient as with an electrode system; in addition, the back reaction between the evolved hydrogen and oxygen gases can take place, which cannot occur in the photoelectrochemical system. This was a problem in early work with  $\text{TiO}_2/\text{Pt}$  photocatalysts [4].

Photocatalytic water splitting has been studied intensively in Japan over the past several decades. A number of photocatalysts, in the form of oxides, nitrides, oxynitrides, and sulfides, have been developed. Especially in the last five years, great progress has been made in preparing highly efficient photocatalysts for water splitting.

A variety of metal oxides have been examined as powder photocatalysts. These materials include transition metal oxides containing metal ions of  $\text{Ti}^{4+}$ ,  $\text{Zr}^{4+}$ ,  $\text{Nb}^{5+}$ , or  $\text{Ta}^{5+}$  with  $d^0$  electronic configuration [17–20] and typical metal oxides having metal ions of  $\text{Ga}^{3+}$ ,  $\text{In}^{3+}$ ,  $\text{Ge}^{4+}$ ,  $\text{Sn}^{4+}$ , or  $\text{Sb}^{5+}$  with  $d^{10}$  electronic configuration [21–24]. Among these, tantalate photocatalysts show the best activity.

Table 1 lists various tantalate photocatalysts for water splitting. These photocatalysts are active even without a cocatalyst such as platinum or NiO because of the high  $E_{\text{CB}}$  level made up from  $\text{Ta}_{5d}$  orbitals. The activity was found to be dependent on  $E_{\text{CB}}$  for the series  $\text{LiTaO}_3$ ,  $\text{NaTaO}_3$  and  $\text{KTaO}_3$ : the higher the  $E_{\text{CB}}$  level is, the higher the yields of  $\text{H}_2$  and  $\text{O}_2$  are [19]. The same tendency was also found for the series  $\text{CaTa}_2\text{O}_6$ ,  $\text{SrTa}_2\text{O}_6$ , and  $\text{BaTa}_2\text{O}_6$  [19]. The deposition of NiO as a cocatalyst often dramatically improved the yields of  $\text{H}_2$  and  $\text{O}_2$ . NiO/ $\text{NaTaO}_3$  is the most active photocatalyst listed in Table 1. The photocatalytic activity of this catalyst increased remarkably with doping of lanthanoid ions, as reported by Kato et al. [20]. An optimized NiO (0.2 wt%)/ $\text{NaTiO}_3\text{:La}$  (2%) photocatalyst showed high activity, with an apparent quantum

yield (QY) of 56% for water splitting. Under illumination with light from a 400-W high pressure mercury lamp,  $\text{H}_2$  and  $\text{O}_2$  evolved at rates of 19.8 and 9.7  $\text{mmol h}^{-1}$ , respectively.

La-doping reduced the particle size and created ordered surface nanosteps on  $\text{NaTaO}_3$  particles [20]. The small particle size with high crystallinity was advantageous in terms of increasing the probability of the reactions of photogenerated electrons and holes with water molecules, rather than recombination. Transmission electron microscope observations and extended X-ray fine structure analyses indicated that the NiO cocatalyst was deposited as ultrafine NiO particles on the edges of the nanostep structures. The  $\text{H}_2$  evolution site of the edge was effectively separated from the  $\text{O}_2$  evolution site of the groove at the surface nanostep structure. This separation is advantageous, especially for water splitting, in order to avoid the back reaction.

Oxide photocatalysts are advantageous in terms of stability and oxygen evolution activity. Recent studies showed that some metal nitrides could also be used for water photo-splitting. Sato et al. reported the first successful metal nitride photocatalyst,  $\beta\text{-Ge}_3\text{N}_4$ , for overall water splitting [25]. The  $\beta\text{-Ge}_3\text{N}_4$  was prepared from  $\text{GeO}_2$  powder by nitridation under  $\text{NH}_3$  atmosphere at 1153 K.  $\beta\text{-Ge}_3\text{N}_4$  alone exhibited little photocatalytic activity for water decomposition, but, when loaded with  $\text{RuO}_2$ , it became photocatalytically active under UV light ( $\lambda < 320 \text{ nm}$ ). The quantum efficiency at 300 nm was ca. 9% for 1%  $\text{RuO}_2$ -loaded  $\beta\text{-Ge}_3\text{N}_4$ .  $\text{N}_2$  evolution, indicative of degradation of the nitride photocatalyst, was observed in the initial stage of reaction at pH 7.0 but was almost entirely suppressed at pH 0. The  $\text{H}_2/\text{O}_2$  production ratio was the stoichiometric ratio of 2, within experimental error, for over 24 h.

Band engineering has been employed in the design of water-splitting photocatalysts in order to improve the use of the visible portion of the solar spectrum. One approach is to dope wide band-gap photocatalysts with metal ions, which create local energy levels within the band gap of the photocatalyst, with corresponding absorption bands lying in the visible spectral range. Kudo et al. codoped  $\text{SrTiO}_3$  with a combination of either

Table 1  
Several alkali metal and alkaline earth tantalate catalysts for water photo-splitting [18,19]

Catalyst	Band gap (eV)	NiO (wt%)	Activity ( $\mu\text{mol h}^{-1}$ )	
			$\text{H}_2$	$\text{O}_2$
$\text{LiTaO}_3$	4.7	None	430	220
$\text{LiTaO}_3$	4.7	0.1	98	52
$\text{NaTaO}_3$	4	None	160	86
$\text{NaTaO}_3$	4	0.05	2180	1100
$\text{KTaO}_3$	3.6	None	29	13
$\text{KTaO}_3$	3.6	0.05	7	3
$\text{CaTa}_2\text{O}_6$	4	None	21	8
$\text{CaTa}_2\text{O}_6$	4	0.1	72	32
$\text{SrTa}_2\text{O}_6$	4.4	None	140	66
$\text{SrTa}_2\text{O}_6$	4.4	0.1	960	490
$\text{BaTa}_2\text{O}_6$	4.1	None	33	15
$\text{BaTa}_2\text{O}_6$	4.1	0.3	629	303
$\text{Sr}_2\text{Ta}_2\text{O}_7$	4.6	None	53	18
$\text{Sr}_2\text{Ta}_2\text{O}_7$	4.6	0.15	1000	480

Photocatalyst: 1.0 g; water: 390 mL; reaction cell: inner irradiation-type quartz cell; light source: 400 W high pressure mercury lamp.

$\text{Sb}^{5+}$  or  $\text{Ta}^{5+}$  and  $\text{Cr}^{3+}$ , and observed  $\text{H}_2$  evolution from an aqueous methanol solution under visible light ( $\lambda > 420 \text{ nm}$ ) [26]. The doping with  $\text{Cr}^{3+}$  created donor levels within the band gap. Codoping with  $\text{Sb}^{5+}$  or  $\text{Ta}^{5+}$  was very necessary to maintain the charge balance, resulting in the suppression of the formation of  $\text{Cr}^{6+}$  ions and oxygen defects in the lattice. Rh-doped  $\text{SrTiO}_3$  also showed activity for  $\text{H}_2$  evolution from an aqueous methanol solution, with a QY of 5.2% at 420 nm. The visible light response was due to the transition from the donor level formed by the Rh ions to the conduction band of  $\text{SrTiO}_3$  [27]. Zou et al. reported a single phase  $\text{In}_{0.9}\text{Ni}_{0.1}\text{TaO}_4$  photocatalyst for overall water splitting [28]. After deposition of Ni/NiO cocatalyst, the material showed photocatalytic activity up to 550 nm, with a QY of 0.66% at 402 nm. Stoichiometric yields of  $\text{H}_2$  and  $\text{O}_2$  were observed for a 400-h period of visible light illumination, with no changes occurring in the catalyst sample.

The local energy levels, created by doping, are always discrete (i.e., narrow) and are thus unsuitable for the migration of photogenerated charge carriers. In addition, the impurity levels often work as recombination centers. A more useful approach is to lift the valence band energy of the wide band-gap photocatalyst. Kudo et al. employed  $\text{Bi}^{3+}$  and  $\text{Sn}^{2+}$  with  $ns^2$  configurations, and  $\text{Ag}^+$  with a  $d^{10}$  configuration, to modify the valence band of oxide photocatalysts [29–31]. They found that  $\text{SnNb}_2\text{O}_6$  was active for  $\text{H}_2$  evolution under visible light, while  $\text{BiVO}_4$  and  $\text{AgNbO}_3$  were active for  $\text{O}_2$  evolution from aqueous silver nitrate solution under visible light. These valence band-controlled photocatalysts showed steep absorption edges in the visible light region, very different from the absorption generated from discrete impurity levels. The photocatalytic activity of  $\text{BiVO}_4$  was much higher than that of commercial  $\text{WO}_3$  with a 2.8-eV band gap, which is a well-known photocatalyst for  $\text{O}_2$  evolution.

Domen et al. reported that a solid solution of GaN and ZnO ( $\text{GaN:ZnO}$ ) could split water into  $\text{H}_2$  and  $\text{O}_2$  stoichiometrically under visible light irradiation, after modification with  $\text{RuO}_2$  cocatalyst [32]. GaN and ZnO are both wide band gap semiconductors, with band gaps of 3.4 and 3.2 eV, respectively. However, the  $\text{GaN:ZnO}$  was yellow colored, with a band gap of 2.58 eV. Density functional theory calculations indicated that the bottom of the conduction band of the  $\text{GaN:ZnO}$  solid solution was mainly composed of 4s and 4p orbitals of Ga, while the top of the valence band consisted of N 2p orbitals, followed by Zn 3d orbitals. The presence of Zn 3d and N 2p electrons in the upper valence band might provide p–d repulsion for the valence band maximum, which resulted in a narrowing of the band gap.  $\text{H}_2$  and  $\text{O}_2$  were found to evolve from the solid solution photocatalyst steadily and stoichiometrically, with negligible  $\text{N}_2$  evolution. The average apparent quantum efficiency was calculated to be 0.14% in the range of 300–480 nm.

Metal sulfides are attractive as photocatalysts with visible light response, though they always encounter the problem of photocorrosion. A representative photocatalyst is Pt/CdS, which is active for  $\text{H}_2$  evolution from aqueous solutions containing sacrificial reagents under visible light irradiation [33]. Recently, Tsuji et al. reported that the  $(\text{AgIn})_x\text{Zn}_{2(1-x)}\text{S}_2$  solid solution

was active for  $\text{H}_2$  evolution from aqueous solution containing sacrificial reagents,  $\text{SO}_3^{2-}$  and  $\text{S}^{2-}$  under visible light irradiation [34]. Loading of the Pt cocatalyst improved the photocatalytic activity. Pt-loaded  $(\text{AgIn})_{0.22}\text{Zn}_{1.56}\text{S}_2$ , with a 2.3-eV band gap, showed the highest activity for  $\text{H}_2$  evolution, and the apparent QY at 420 nm was 20%.  $\text{H}_2$  gas evolved at a rate of  $3.3 \text{ L m}^{-2} \text{ h}^{-1}$  under AM 1.5 simulated sunlight. Very recently, a  $\text{ZnS-AgInS}_2\text{-CuInS}_2$  solid solution,  $(\text{CuAg})_{0.15}\text{In}_{0.3}\text{Zn}_{1.4}\text{S}_2$ , was reported to split water up to about 650 nm [35]. Deposition of Ru cocatalyst improved the photocatalytic activity. Under AM 1.5 simulated sunlight, the hydrogen evolution rate was  $8.2 \text{ L m}^{-2} \text{ h}^{-1}$  from aqueous solution containing sacrificial reagents, corresponding to a solar energy conversion efficiency of ca. 2.4%. The activity remained comparatively stable over 20 h when the reaction solution was replaced periodically with fresh solution.

Overall water splitting was also carried out in a combined system by a two-photon process under visible light. The combined system consisted of an  $\text{H}_2$ -evolving photocatalyst, an  $\text{O}_2$ -evolving photocatalyst, and a redox couple as a charge mediator. Both Sayama et al. and Kudo et al. have carried out studies in this field [36,37]. The  $(\text{Pt/SrTiO}_3:\text{Rh})\text{-(BiVO}_4\text{)-Fe}^{3+}/\text{Fe}^{2+}$  couple system was able to respond to visible light up to 520 nm, with an apparent QY of 0.3% at 440 nm [37].

### 2.3. Perspectives

The ultimate target of water splitting is to provide clean  $\text{H}_2$  fuel through the utilization of solar energy. Considerable efficiencies for solar water splitting have been reported for the photovoltaic–photoelectrolytic device of Khaselev and Turner [14] and for the photovoltaic–electrolytic device of Licht [38]. The record efficiency of 18.3%, achieved on a  $\text{AlGaAs/Si-RuO}_2/\text{Pt}$  system, is very encouraging. However, these systems are so expensive that the cost of the hydrogen fuel produced would not be competitive with other regenerative types of energy. Heterogeneous photocatalysis could provide a low-cost route for production of  $\text{H}_2$  fuel, if the photocatalyst were able to utilize solar energy efficiently. Recent studies on  $\text{NiO/NaTaO}_3:\text{La}$  have proven that highly efficient water splitting is actually possible with a particulate photocatalyst system. The problem is to find a way to split water efficiently under visible light.  $(\text{CuAg})_{0.15}\text{In}_{0.3}\text{Zn}_{1.4}\text{S}_2$  is a very promising photocatalyst. The photocatalytic activity of this material could be higher if a better preparation method were found with which the density of defects and impurities is lowered. If such a preparation method were found, this material might have applications in the production of hydrogen gas from by-products, such as hydrogen sulfide and sulfur dioxide, of hydrogenation and flue-gas desulfurization processes at chemical plants.

A desirable photocatalyst for solar water splitting should have a photo-response up to 600 nm, a lifetime of over one year in continuous operation, and an overall solar energy conversion efficiency of at least 15%. These parameters can very possibly be achieved, if sufficient knowledge is accumulated on the determining factors of photocatalytic activity, such as composition, structure, particle size, defect density, surface structure,



and cocatalyst, etc. High throughput methods should be established for the preparation and evaluation of photocatalysts.

### 3. Photocatalytic environmental cleanup

#### 3.1. General knowledge

Ever since the report of the use of illuminated  $\text{TiO}_2$  powder to decompose cyanide in water 1977 [39], there has been increasing interest in the environmental applications of photocatalysis. This work has typically used  $\text{TiO}_2$ , which is an ideal photocatalyst, because it is highly stable chemically, and the photogenerated holes are highly oxidizing. In addition, it is relatively inexpensive and non-toxic. As shown in Fig. 3, the redox potential for photogenerated holes is +2.53 V versus the standard hydrogen electrode (SHE) in pH 7 aqueous solution. After reaction with water, these holes can produce hydroxyl radicals ( $\bullet\text{OH}$ ), whose redox potential ( $\bullet\text{OH}/\text{OH}^-$ ) is only slightly decreased and is in fact still more positive than that for ozone ( $\text{O}_3/\text{O}_2$ ). The redox potential for conduction band electrons is  $-0.52$  V, which is negative enough to reduce dioxygen to superoxide. All of the photoproducted species, including holes,  $\bullet\text{OH}$  radicals,  $\text{O}_2^-$ ,  $\text{H}_2\text{O}_2$  and  $\text{O}_2$ , play important roles in the photocatalytic reaction mechanisms.

Photocatalytic reactions mainly occur at or very close to the surface of an illuminated photocatalyst. However, recent studies have shown that photocatalytic reactions can also occur at distances remote (tens of micrometers) from the illuminated surface, through the diffusion of reactive species in air [40,41] or solution phase [42], or through the diffusion of reactive species on the surface [43]. These discoveries are important for the design of photocatalytic systems.

Another intrinsic property of  $\text{TiO}_2$  is the UV-induced superhydrophilicity at surface, i.e., the water contact angle can approach  $0^\circ$  on an illuminated  $\text{TiO}_2$  surface [44]. This property is very advantageous for a number of applications, including anti-fogging, anti-beading, and the so-called self-cleaning process, which employs natural rainfall and sunlight to maintain the surface clean [40]. Several mechanisms have been proposed

for the photo-induced hydrophilic conversion phenomenon, for example, the photo-induced production of  $\text{O}_2$  defects [46], and photo-induced reconstruction of surface hydroxyl groups [47]. There has also been the invocation of the more traditional mechanism of photocatalysis, i.e., the superhydrophilicity is merely caused by the photocatalytic decomposition of organic contaminants that cause the surface to be hydrophobic. However, it is necessary to take into account the fact that some oxides, such as  $\text{SrTiO}_3$ , have photocatalytic oxidation ability but do not become hydrophilic by means of UV illumination; in addition, other oxides, such as  $\text{WO}_3$ , show a photo-induced hydrophilic conversion but do not exhibit photocatalytic activity [48]. Thus, one of the unique aspects of  $\text{TiO}_2$  is that there are actually two distinct photo-induced phenomena, i.e., the photocatalytic phenomenon and the photo-induced superhydrophilic phenomenon.

#### 3.2. Applications in environmental cleanup

Extensive studies have been carried out on the environmental applications of immobilized  $\text{TiO}_2$  photocatalysts, i.e., those in which nanoparticles have been formed into thin films. We have focused our attention on the low-intensity range of UV illumination, from  $1 \mu\text{W cm}^{-2}$  to  $1 \text{mW cm}^{-2}$  in our studies, since the ultraviolet light in direct sunlight is generally  $2\text{--}3 \text{mW cm}^{-2}$  in Japan, and that in a reasonably well-lit room is approximately  $1 \mu\text{W cm}^{-2}$  [10]. Selected results will be described briefly below; most are closely related to practical applications.

The first example we describe here is the removal of indoor odors by immobilized  $\text{TiO}_2$  films under weak UV illumination. Odors that are objectionable to humans are due to compounds that are present only on the order of 10 parts per million by volume (ppmv). We found that, at these concentrations, low-intensity UV light ( $1 \mu\text{W cm}^{-2}$ ) was sufficient to decompose such compounds when  $\text{TiO}_2$  photocatalysts were present. Actually, the QY for a simple photocatalytic reaction, e.g., 2-propanol oxidation, on a  $\text{TiO}_2$  film in ambient air, reached a constant maximum value when the light intensity was extremely low, as shown in Fig. 4a [49]. The maximum QY observed was  $\sim 28\%$  for 1000 ppmv 2-propanol under tens of  $\text{nW cm}^{-2}$  UV illumination. This value is dependent upon details of the film preparation and thus is different from film to film. The reported maximum QY for acetaldehyde photocatalytic decomposition was even greater than 100%, due to the existence of a radical chain-type process [50]. Thus, it is even possible to remove noxious pollutants such as this in indoor air with  $\text{TiO}_2$ -containing wallpaper under the illumination of fluorescent lamps [10].

The second example we show here is the bactericidal effect of  $\text{TiO}_2$  under low-intensity UV illumination. In a typical experiment,  $150 \mu\text{L}$  of an *Escherichia coli* suspension, containing  $3 \times 10^4$  cells, was placed on an illuminated  $\text{TiO}_2$ -coated glass plate ( $1 \text{mW cm}^{-2}$ ). Under these conditions, there were no surviving cells after only 1 h of illumination [42]. In contrast, after 4 h under UV illumination without a  $\text{TiO}_2$  film, only 50% of the cells were killed (Fig. 4b). In addition, the dead cells were completely decomposed by the  $\text{TiO}_2$  photocatalyst [51].

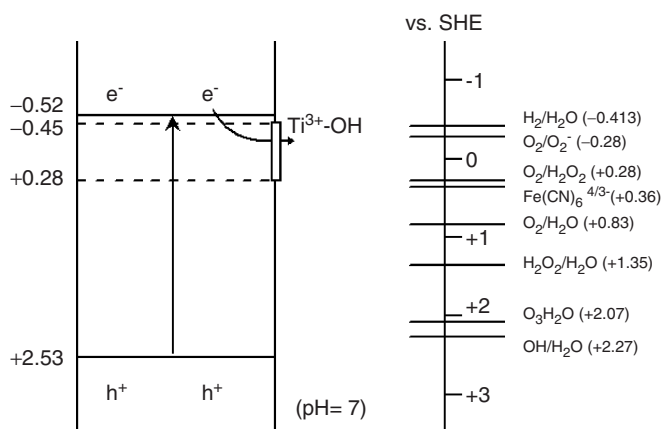


Fig. 3. Schematic diagram showing the potentials for various redox processes occurring on the  $\text{TiO}_2$  surface at pH 7 [9].

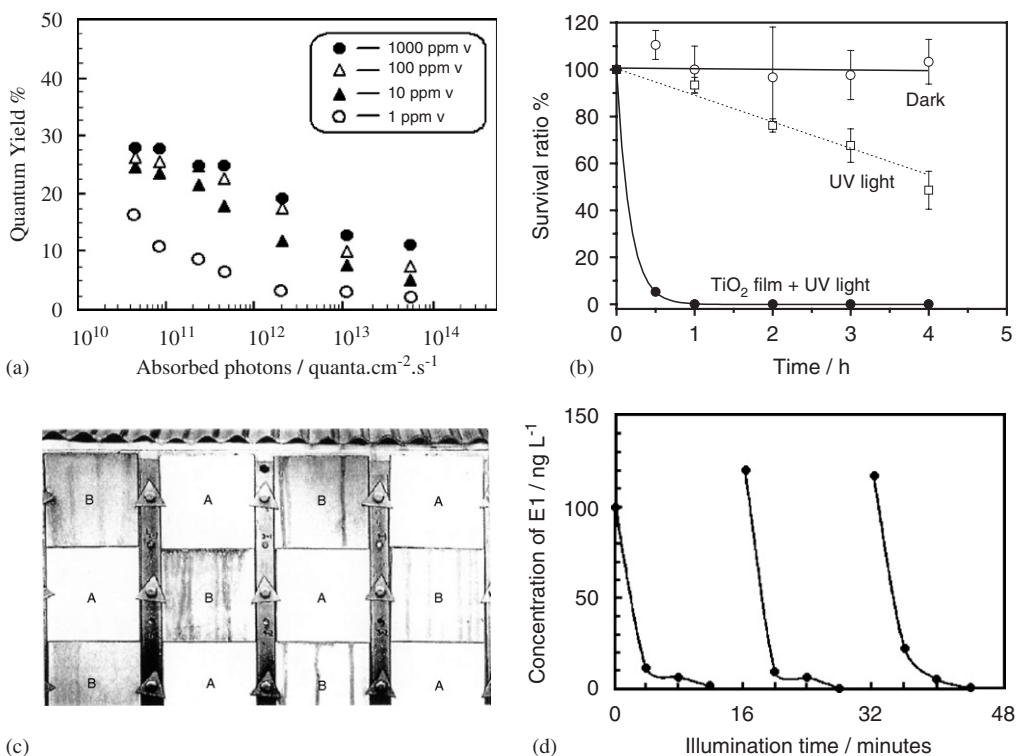


Fig. 4. (a) Quantum yield dependence on absorbed photons at various initial 2-propanol concentrations [44]. (b) Survival ratio of *Escherichia coli* in the liquid film with and without a TiO<sub>2</sub> thin film under black light illumination (1 mW cm<sup>-2</sup>) and with a TiO<sub>2</sub> thin film in the dark [37]. (c) Photograph showing alternating self-cleaning (A) and ordinary (B) exterior wall tiles that have been placed so that water from a corrugated metal roof runs off onto the wall [40]. (d) Concentration change of E1 in discharged water from a sewage treatment plant during photocatalysis [50]. The measurement was repeated three times (UV light intensity, 1.2 mW cm<sup>-2</sup>; water temperature, 15 °C).

In the indoor environment, UV photons are available on levels of  $\sim 1 \mu\text{W cm}^{-2}$ . As studied by Sunada et al., the antibacterial action of TiO<sub>2</sub> film was negligible at this UV intensity. However, when metallic Cu clusters were applied to the TiO<sub>2</sub> surface, clear evidence for antibacterial action was observed, even under indoor illumination [52].

The third example we show here is that of a self-cleaning TiO<sub>2</sub> surface under low-intensity UV illumination. In one study, we found that organic compounds, such as octadecane, glycerol trioleate, and poly(ethylene glycol) (MW 500,000), could be decomposed completely on the TiO<sub>2</sub> surface under low-intensity UV illumination (1 mW cm<sup>-2</sup>) at significant rates, with the evolution of CO<sub>2</sub> as the only detectable gas-phase product [53]. This observation is important, because it shows that the TiO<sub>2</sub> surface has the ability to self-regenerate. The soiling of building exteriors is closely related to the contamination of oily organic substances on the surface, to which airborne dust adheres. If the exterior surfaces of buildings are covered with TiO<sub>2</sub> coatings, adsorbed organic contaminants can be decomposed by the photocatalytic action of TiO<sub>2</sub> when illuminated with sunlight, while the superhydrophilic action of TiO<sub>2</sub> facilitates the spread and flow of rainwater on surface. As a result, rainwater can effectively wash off dust, sand, and even organic contaminants. This idea was first examined by TOTO Ltd. of Japan on ceramic tiles. Ordinary tiles and TiO<sub>2</sub>-coated tiles were placed outdoors on an exterior wall that was located under a corrugated roof

and was exposed to sunlight and rainwater. After six months, the contrast was striking between the ordinary tiles, on which soiling was very conspicuous, and the TiO<sub>2</sub>-coated tiles, which were not soiled at all (Fig. 4c) [45].

The fourth example we show here is the photocatalytic decomposition of endocrine-disrupter chemicals (EDCs) in water. Natural estrogens of 17 $\beta$ -estradiol (E2) and estron (E1) are basic female sex hormones and are well known to exhibit potent estrogenic activity, even at very low concentrations ( $\sim 10^{-9}$  M), and have been suggested to affect the propagation of wildlife. We found that the two compounds (E1 and E2) dissolved in water could be decomposed completely by TiO<sub>2</sub> photocatalysts under weak illumination [54]. Most importantly, the intermediates produced during photocatalytic reactions did not exhibit any potent estrogenic activity in the treated water. We designed a photocatalytic reactor using TiO<sub>2</sub>-modified-PTFE mesh sheets as photocatalysts, and applied this to treat the water discharged from the Kitano sewage treatment plant at the Tama River near Tokyo. Concentrations of E1 and E2 in the discharged water were 140 and 15 ng L<sup>-1</sup>, respectively. Under UV illumination (1.2 mW cm<sup>-2</sup>), about 90% of the initial E1 was decomposed in a short time, with very good reproducibility, as shown in Fig. 4d [55]. Thus, TiO<sub>2</sub> photocatalysis can be applied in water treatment as a novel method for removing natural and synthetic estrogens effectively, without generating biologically active intermediates.

Table 2  
Selected applications of photocatalysis

Property	Category	Application
Self-cleaning	Materials for residential and office buildings	Exterior tiles, kitchen and bathroom components, interior furnishings, plastic surfaces, aluminum siding, building stone and curtains, window blinds
	Indoor and outdoor lamps and related systems	Translucent paper for indoor lamp covers, coatings on fluorescent lamps and highway tunnel lamp cover glass
	Materials for roads	Tunnel wall, soundproofed wall, traffic signs and reflectors
	Others	Tent material, spray coatings for cars
Air purification	Indoor air cleaners	Room air cleaner, air conditioner, and interior air cleaner for factories
	Outdoor air purifiers	Concrete for highways, roadways and footpaths, tunnel walls, soundproofed walls, and building walls
Water purification	Drinking water	River water, ground water, lakes and water-storage tanks
	Others	Industrial wastewater, agricultural wastewater, hot spring water, drainage water, pool water, fish feeding tanks,
Self-sterilizing	Hospital	Tiles and coatings to cover the floor, walls and ceiling of operating rooms, silicone rubber for medical catheters, and hospital garments and uniforms
	Others	Public rest rooms, bathrooms, pet-breeding rooms

The commercialization of TiO<sub>2</sub>-based photocatalytic products commenced in the mid-1990s in Japan. However, this industry has grown very quickly, and its market reached ca. 50 billion Japanese yen in Japan in 2004. More than 2000 companies have joined in this new industry, whose products have covered self-cleaning, air purification, water purification, and bactericidal applications, as shown in Table 2. The self-cleaning exterior construction materials, such as tiles, glass, plastic films, coatings, etc., are the most popular products. The market of air cleaners has grown very rapidly over the past two years because of the increasing concern of the public for indoor air pollutants such as formaldehyde, toluene, and acetaldehyde, etc. Some purification facilities for underground water, hot spring water, etc., have also appeared on the market.

Some new applications of TiO<sub>2</sub> photocatalysis have been proposed recently. Tatsuma et al. employed TiO<sub>2</sub>-WO<sub>3</sub> composite coatings in the photoelectrochemical anti-corrosion of steel [56,57]. The coating even worked in dark, because of the energy storage property of WO<sub>3</sub>. Applications of remote photocatalysis in microfabrication have also been proposed [58,59].

### 3.3. Future perspectives

One of the major challenges for the scientific community involved in photocatalytic research is to increase the spectral sensitivity of photocatalysts to visible light, which composes the largest part of solar radiation. Anatase TiO<sub>2</sub>, which is the most photoactive phase of TiO<sub>2</sub>, only absorbs ultraviolet light with wavelengths shorter than 380 nm. However, the UV part of direct sunlight is generally in the range of 2–3 mW cm<sup>-2</sup> in Japan. The content of ultraviolet light in indoor illumination is significantly smaller than that in sunlight, because the fluorescent lamp mainly emits visible light. Asahi et al. recently reported significant red shifts (up to 540 nm) of the spectral limit

of the photoactivity of TiO<sub>2</sub> photocatalysts doped with nitrogen [60]. They interpreted such results in terms of band gap narrowing due to mixing of the p states of the dopants with O 2p states forming the valence band of TiO<sub>2</sub>. A similar conclusion has also been reached by Ohno et al. for the spectral changes observed for S-doped TiO<sub>2</sub> [61].

One may worry about the photocatalytic oxidation powder of these anion-doped TiO<sub>2</sub>, especially the power to yield hydroxyl radicals in visible light, since the impurity levels are above the valence band edge of pure TiO<sub>2</sub>. However, our recent studies in phenol degradation could relieve this worry, since the quantum efficiency of phenol degradation in visible light is only slightly lower than that in UV light, when N-doped TiO<sub>2</sub> is used as the photocatalyst [62]. Moreover, the quantum efficiency of phenol degradation for N-doped TiO<sub>2</sub> is also only slightly lower than that of pure TiO<sub>2</sub> in UV light. The present problem for the anion-doped TiO<sub>2</sub> photocatalysts is that their absorption coefficients for the visible light are always very low, which limits the photocatalytic efficiency in that wavelength region. Much effort must be devoted to overcome this obstacle.

One must keep in mind the fact that photocatalytic environmental cleanup is only suitable for low-level pollutants, since the amount of ultraviolet photons is limited in both solar light and indoor illumination. In some fields, such as the outdoor self-cleaning application, the UV photons in solar light might be sufficient. However, for water purification, the level of UV photons in solar light is too low to perform effective photocatalytic cleanup, compared to the concentration of pollutants. This is the reason why photocatalysis is only considered as an auxiliary to biological remediation and other advanced oxidation process at the present stage. The future of photocatalytic environmental cleanup is dependent on how efficiently the photocatalyst can use solar light.

## Acknowledgment

This work was supported by the a Grant-in Aid for Scientific Research on Priority Areas (417) from the Ministry of Education, Culture, Sports, Science and Technology (MEXT) of the Japanese Government, and by the Core Research for Evolutional Science and Technology (CREST) program of the Japan Science and Technology (JST) Agency.

## References

- [1] Fujishima A, Honda K, Kikuchi S. Photosensitized electrolytic oxidation on TiO<sub>2</sub> semiconductor electrode. *J Chem Soc Japan (Kogyo Kagaku Zasshi)* 1969;72:108–9.
- [2] Fujishima A, Honda K. Electrochemical photolysis of water at a semiconductor electrode. *Nature* 1972;238:37–8.
- [3] Kawai T, Sakata T. Hydrogen evolution from water using solid carbon and light energy. *Nature* 1979;282:283–4.
- [4] Sato S, White JM. Photodecomposition of water over Pt/TiO<sub>2</sub> catalyst. *Chem Phys Lett* 1980;72:83–6.
- [5] Kawai T, Sakata T. Conversion of carbohydrate into hydrogen fuel by a photocatalytic process. *Nature* 1980;286:474–6.
- [6] Fox MA, Dulay MT. Heterogeneous photocatalysis. *Chem Rev* 1993;93:341–57 and references therein.
- [7] Hoffmann MR, Martin ST, Choi W, Bahnemann DW. Environmental applications of semiconductor photocatalysis. *Chem Rev* 1995;95:69–96.
- [8] Linsebigler AL, Lu G, Yates JT. Photocatalysis on TiO<sub>2</sub> surface: principles, mechanisms, and selected results. *Chem Rev* 1995;95:735–58.
- [9] Fujishima A, Tryk DA, Rao TN. Titanium dioxide photocatalysis. *J Photochem Photobiol C: Photochem Rev* 2000;1:1–21.
- [10] Fujishima A, Hashimoto K, Watanabe T. TiO<sub>2</sub> photocatalysis: fundamentals and applications. Tokyo: BKC, Inc.; 1999.
- [11] Fujishima A, Zhang X, TiO<sub>2</sub> photocatalysis: present situation and future perspectives, C. R. *Chimie* 2006;9:750–60.
- [12] Fujishima A, Kohayakawa K, Honda K. Hydrogen production under sunlight with an electrochemical photocell. *J Electrochem Soc* 1975;122:1487–9.
- [13] Fujishima A, Tryk DA. Photoelectrochemical conversion. In: Honda K, editor. *Functionality of molecular systems*, vol. 2. Tokyo: Springer; 1999. p. 196–224.
- [14] Khaselev O, Turner JA. A monolithic photovoltaic–photoelectrochemical device for hydrogen production via water splitting. *Science* 1998;280:425–7.
- [15] Bard AJ. Photoelectrochemistry and heterogeneous photocatalysis at semiconductors. *J Photochem* 1979;10:59–75.
- [16] Bard AJ. Photoelectrochemistry. *Science* 1980;207:139–44.
- [17] Domen K, Kondo JN, Hara M, Takata T. Photo- and mechano-catalytic overall water splitting reactions to from hydrogen and oxygen on heterogeneous catalysts. *Bull Chem Soc Japan* 2000;73:1307–31.
- [18] Kudo A, Kato H, Tsuji I. Strategies for the development of visible-light-driven photocatalysts for water splitting. *Chem Lett* 2004;33:1534–9.
- [19] Kato H, Kudo A. Photocatalytic water splitting into H<sub>2</sub> and O<sub>2</sub> over various tantalate photocatalysts. *Catalysis Today* 2003;78:561–9.
- [20] Kato H, Asakura K, Kudo A. Highly efficient water splitting into H<sub>2</sub> and O<sub>2</sub> over Lanthanum-doped NaTaO<sub>3</sub> photocatalysts with high crystallinity and surface nanostructure. *J Am Chem Soc* 2003;125:3082–9.
- [21] Ikarashi K, Sato J, Saito N, Nishiyama H, Inoue Y. Photocatalysis for water decomposition by RuO<sub>2</sub>-dispersed ZnGa<sub>2</sub>O<sub>4</sub> with d<sup>10</sup> configuration. *J Phys Chem B* 2002;106:9048–53.
- [22] Sato J, Saito N, Nishiyama H, Inoue Y. Photocatalytic activity for water decomposition of Indates with octahedrally coordinated d<sup>10</sup> configuration. 1. Influence of preparation conditions on activity. *J Phys Chem B* 2003;107:7965–9.
- [23] Sato J, Kobayashi H, Saito N, Nishiyama H, Inoue Y. Photocatalytic activity for water decomposition of RuO<sub>2</sub>-dispersed Zn<sub>2</sub>GeO<sub>4</sub> with d<sup>10</sup> configuration. *J Phys Chem B* 2004;108:4369–75.
- [24] Sato J, Saito N, Nishiyama H, Inoue Y. New photocatalyst group for water decomposition of RuO<sub>2</sub>-loaded p-block metal (In, Sn, and Sb) oxides with d<sup>10</sup> configuration. *J Phys Chem B* 2001;105:6061–3.
- [25] Sato J, Saito N, Yamada Y, Maeda K, Takata T, Kondo JN, et al. RuO<sub>2</sub>-loaded β-Ge<sub>3</sub>N<sub>4</sub> as a non-oxide photocatalyst for overall water splitting. *J Am Chem Soc* 2005;127:4150–1.
- [26] Ishii T, Kato H, Kudo A. H<sub>2</sub> evolution from an aqueous methanol solution on SrTiO<sub>3</sub> photocatalysts codoped with chromium and tantalum ions under visible light irradiation. *J Photochem Photobiol A: Chem* 2004;163:181–6.
- [27] Konta R, Ishii T, Kato H, Kudo A. Photocatalytic activities of noble metal ion-doped SrTiO<sub>3</sub> under visible light irradiation. *J Phys Chem B* 2004;108:8992–5.
- [28] Zou Z, Ye J, Sayama K, Arakawa H. Direct splitting of water under visible light irradiation with an oxide semiconductor photocatalyst. *Nature* 2001;414:625–7.
- [29] Hosogi Y, Tanabe K, Kato H, Kobayashi H, Kudo A. Energy structure and photocatalytic activity of niobates and tantalates containing Sn(II) with a 5s<sup>2</sup> electron configuration. *Chem Lett* 2004;33:28–9.
- [30] Kudo A, Omori K, Kato H. A novel aqueous process for preparation of crystal form-controlled and highly crystalline BiVO<sub>4</sub> powder from layered vanadates at room temperature and its photocatalytic and photophysical properties. *J Am Chem Soc* 1999;121:11459–67.
- [31] Kato H, Kobayashi H, Kudo A. Role of Ag<sup>+</sup> ions for band structures and photocatalytic properties of AgMO<sub>3</sub> (M: Ta and Nb) with the perovskite structure. *J Phys Chem B* 2002;106:12441–7.
- [32] Maeda K, Takata T, Hara M, Saito N, Inoue Y, Kobayashi H, et al. GaN: ZnO solid solution as a photocatalyst for visible-light-driven overall water splitting. *J Am Chem Soc* 2005;127:8286–7.
- [33] Matsumura M, Furukawa S, Saho Y, Tsubomura H. Cadmium sulfide photocatalyzed hydrogen production from aqueous solutions of sulfite: effect of crystal structure and preparation method of the catalyst. *J Phys Chem* 1985;89:1327–9.
- [34] Tsuji I, Kato H, Kobayashi H, Kudo A. Photocatalytic H<sub>2</sub> evolution reaction from aqueous solutions over band structure-controlled (AgIn)<sub>x</sub>Zn<sub>2(1-x)</sub>S<sub>2</sub> solid solution photocatalysts with visible-light response and their surface nanostructures. *J Am Chem Soc* 2004;126:13406–13.
- [35] Tsuji I, Kato H, Kudo A. Visible-light-induced H<sub>2</sub> evolution from an aqueous solution containing sulfide and sulfite over a ZnS–CuInS<sub>2</sub>–AgInS<sub>2</sub> solid-solution photocatalyst. *Angew Chem Int Ed* 2005;44:3565–8.
- [36] Sayama K, Mukasa K, Abe R, Abe Y, Arakawa H. *Chem Commun* 2001; 2416–7.
- [37] Kato H, Hori M, Konta R, Shimodaira Y, Kudo A. Construction of Z-scheme type heterogeneous photocatalysis systems for water splitting into H<sub>2</sub> and O<sub>2</sub> under visible light irradiation. *Chem Lett* 2004;33:1348–9.
- [38] Licht S. Solar water splitting to generate hydrogen fuel: photothermal electrochemical analysis. *J Phys Chem B* 2003;107:4253–60.
- [39] Frank SN, Bard AJ. Heterogeneous photocatalytic oxidation of cyanide ion in aqueous solution at TiO<sub>2</sub> powder. *J Am Chem Soc* 1977;99:303–4.
- [40] Tatsuma T, Tachibana S, Miwa T, Tryk DA, Fujishima A. Remote bleaching of methylene blue by UV irradiated TiO<sub>2</sub> in the gas phase. *J Phys Chem B* 1999;103:8033–5.
- [41] Tatsuma T, Tachibana S, Fujishima A. Remote oxidation of organic compounds by UV-irradiated TiO<sub>2</sub> via the gas phase. *J Phys Chem B* 2001;105:6987–92.
- [42] Kikuchi Y, Sunada K, Iyoda T, Hashimoto K, Fujishima A. Photocatalytic bactericidal effect of TiO<sub>2</sub> thin films: dynamic view of the active oxygen species responsible for the effect. *J Photochem Photobiol A: Chem* 1997;106:51–6.
- [43] Haick H, Paz Y. Remote photocatalytic activity as probed by measuring the degradation of self-assembled monolayers anchored near microdomains of titanium dioxide. *J Phys Chem B* 2001;105:3045–51.
- [44] Wang R, Hashimoto K, Fujishima A, Chikuni M, Kojima E, Kitamura A, et al. Light-induced amphiphilic surfaces. *Nature* 1997;388:431–2.



- [45] Wang R, Hashimoto K, Fujishima A, Chikuni M, Kojima E, Kitamura A. et al. Photogeneration of highly amphiphilic TiO<sub>2</sub> surfaces. *Adv Mater* 1998;10:135–8.
- [46] Wang R, Sakai N, Fujishima A, Watanabe T, Hashimoto K. Studies of surface wettability conversion on TiO<sub>2</sub> single crystal surfaces. *J Phys Chem B* 1999;103:2188–94.
- [47] Sakai N, Fujishima A, Watanabe T, Hashimoto K. Quantitative evaluation of the photoinduced hydrophilic conversion properties of TiO<sub>2</sub> thin film surfaces by the reciprocal of contact angle. *J Phys Chem B* 2003;107:1028–35.
- [48] Miyauchi M, Nakajima A, Watanabe T, Hashimoto K. Photocatalysis and photoinduced hydrophilicity of various metal oxide thin films. *Chem Mater* 2002;14:2812–6.
- [49] Ohko Y, Hashimoto K, Fujishima A. Kinetics of photocatalytic reactions under extremely low-intensity UV illumination on titanium dioxide thin films. *J Phys Chem A* 1997;101:8057–62.
- [50] Ohko Y, Tryk DA, Hashimoto K, Fujishima A. Autooxidation of acetaldehyde initiated by TiO<sub>2</sub> photocatalysis under weak UV illumination. *J Phys Chem B* 1998;102:2699–704.
- [51] Sunada K, Watanabe T, Hashimoto K. Studies on photokilling of bacteria on TiO<sub>2</sub> thin film. *J Photochem Photobiol A: Chem* 2003;156:227–33.
- [52] Sunada K, Watanabe T, Hashimoto K. Bactericidal activity of copper-deposited TiO<sub>2</sub> thin film under weak UV light illumination. *Environ Sci Technol* 2003;37:4785–9.
- [53] Minabe T, Tryk DA, Sawunyama P, Kikuchi Y, Fujishima A, Hashimoto K. TiO<sub>2</sub>-mediated photodegradation of liquid and solid organic compounds. *J Photochem Photobiol A: Chem* 2000;137:53–62.
- [54] Ohko Y, Iuchi K, Niwa C, Tatsuma T, Nakashima T, Iguchi T. et al. 17 $\beta$ -estradiol degradation by TiO<sub>2</sub> photocatalysis as a means of reducing estrogenic activity. *Environ Sci Tech* 2002;36:4175–81.
- [55] Nakashima T, Ohko Y, Kubota Y, Fujishima A. Photocatalytic decomposition of estrogens in aquatic environment by reciprocating immersion of TiO<sub>2</sub>-modified polytetrafluoroethylene mesh sheets. *J Photochem Photobiol A: Chem* 2003;160:115–20.
- [56] Tatsuma T, Saitoh S, Ohko Y, Fujishima A. TiO<sub>2</sub>-WO<sub>3</sub> photoelectrochemical anticorrosion system with an energy storage ability. *Chem Mater* 2001;13:2838–42.
- [57] Tatsuma T, Saitoh S, Ngaotrakanwivat P, Ohko Y, Fujishima A. Energy storage of TiO<sub>2</sub>-WO<sub>3</sub> photocatalysis systems in the gas phase. *Langmuir* 2002;18:7777–9.
- [58] Tatsuma T, Kubo W, Fujishima A. Patterning of solid surfaces by photocatalytic lithography based on the remote oxidation effect of TiO<sub>2</sub>. *Langmuir* 2002;18:9632–4.
- [59] Kubo W, Tatsuma T, Fujishima A, Kobayashi H. Mechanisms and resolution of photocatalytic lithography. *J Phys Chem B* 2004;108:3005–9.
- [60] Asahi R, Morikawa T, Ohwaki T, Aoki K, Taga Y. Visible-light photocatalysis in nitrogen-doped titanium oxides. *Science* 2001;293:269–71.
- [61] Ohno T, Mitsui T, Matsumura M. Photocatalytic activity of S-doped TiO<sub>2</sub> photocatalyst under visible light. *Chem Lett* 2003;32:364–5.
- [62] Emeline AV, Zhang X, Jin M, Murakami T, Fujishima A. Application of the “black body” like reactor for measurements of the quantum yield of photochemical reactions in heterogeneous systems. *J Phys Chem B* 2006;110:7409–13.